Available online at www.sciencedirect.com
SCIENCE DIRECT®
ELSEVIER
Advances in Space Research 37 (2006) 315–322
ADVANCES IN SPACE RESEARCH (a COSPAR publication)
www.elsevier.com/locate/asr

HEUVAC: A new high resolution solar EUV proxy model

Philip G. Richards [a,*], Thomas N. Woods [b], William K. Peterson [b]

[a] Computer Science Department, University of Alabama in Huntsville, 301 Sparkman Drive, Huntsville, AL 35899, United States
[b] Laboratory for Atmospheric and Space Physics, University of Colorado, Boulder, CO, United States

Received 24 October 2004; received in revised form 21 May 2005; accepted 20 June 2005

Abstract

This paper presents a new high-resolution version of the solar EUV irradiance model for aeronomic calculations (HEUVAC) that is designed to facilitate comparisons with measured spectra and enable more accurate calculations of ionization rates, airglow emission rates, and photoelectron calculations. The HEUVAC model bins can range from 0.1 to 100 nm and extends the EUV model below 5 nm. The new solar EUV irradiance calculations with the high resolution irradiance model show good agreement with the most recent solar EUV irradiance measurements from the solar EUV experiment (SEE) instrument on the thermosphere, ionosphere, mesosphere, energetics, and dynamics satellite. Also, photoelectron fluxes calculated from both the SEE measured and EUVAC modeled solar EUV irradiances agree well with photoelectron flux measurements by the FAST satellite. The good agreement of the EUVAC and SEE derived photoelectron fluxes with the FAST measured fluxes at solar maximum lends support to an earlier finding that the previous reference solar EUV irradiances from the Atmosphere Explorer measurements need to be adjusted upward by a factor of 2–3 below 25 nm wavelength. This result is important for remote sensing of the ionosphere and thermosphere because, as this paper shows, the airglow emission rates calculated using the SEE and HEUVAC models are 50% higher than those based on earlier solar EUV irradiance models. The calculations also show that for solar maximum conditions on 21 April 2002, most of the degradation of the escaping photoelectron flux takes place below 1000 km altitude.

Keywords: Solar EUV flux; Photoelectron flux; Ionization; Airglow

1. Introduction

The solar EUV irradiance is a key input to the thermosphere. It is not only responsible for creating the ionosphere but also numerous airglow emissions that are important for diagnosing the state of the upper atmosphere.

Early rocket measurements during the 1960s and early 1970s culminated in the production of the F74113 solar reference spectrum that was used extensively along with Atmosphere Explorer-C satellite data to develop the chemical scheme that was highly successful in explaining the aeronomy of the ionosphere and thermosphere. The F74113 reference spectrum covered the wavelength range from 1.4 to 200 nm. A new solar minimum reference spectrum called SC#21REFW was developed following an extensive set of measurements on the Atmosphere Explorer-E satellite from solar minimum in mid 1977 until solar maximum in 1980 and a 1979 rocket measurement (Hinteregger et al., 1981). The SC#21REFW spectrum covered the wavelength range from 1.8 to 200 nm. Warren et al. (1998a,b) and Woods et al. (2005) present a detailed analysis of these reference spectra.

This paper compares model solar EUV irradiances with measurements from the SEE instrument on the thermosphere, ionosphere, mesosphere, energetics, and dynamics (TIMED) satellite. The instrument and the

* Corresponding author. Tel.: +1 202 358 0894; fax: +1 202 358 3987.
E-mail address: richards@cs.uah.edu (P.G. Richards).

0273-1177/$30 © 2005 COSPAR. Published by Elsevier Ltd. All rights reserved.
doi:10.1016/j.asr.2005.06.031

SEE observations have been described by Woods et al. (2003, 2004, 2005). The SEE experiment consists of two instruments. The EUV grating spectrometer (EGS) measures the region from 27 to 194 nm at 0.4 nm resolution. The XUV photometer system (XPS) has nine silicon photodiodes with thin film filters. The XPS is a broadband system with each filter having a spectral bandpass of about 7 nm. The wide band pass of the XPS leads to an important complication: in order to produce a high resolution spectrum below 27 nm, it is necessary to assume a reference spectrum with a particular shape. However, this region of the EUV spectrum is the least well characterized, particularly during solar flares when the shape of the spectrum may be highly variable. This paper uses the non-flare version 8 data that are given at 1 nm resolution over the range 0.5–193.5 nm.

Solar irradiance proxy models are needed because there are large periods when there were no reliable measurements and because they are a convenient input to ionospheric models. Lean et al. (2003) provided an excellent summary of the current state of solar EUV irradiance modeling. They also compared the performance of three empirical models to the NRLEUV first principles model. The three empirical models were: (1) the SERF1 or HFG model; the first EUV model adopted by the SCOSTEP Solar Electromagnetic Radiation Flux (SERF) Study project. (Hinteregger et al., 1981); (2) the SOLAR2000 model (Tobiska et al., 2000); (3) the EUVAC model (Richards et al., 1994). The NRLEUV model, which is based on the physical properties of the solar atmosphere, has been developed over a number of years by Lean et al. (1982, 2003), Fontenla et al. (1999) and Warren et al. (1998a,b, 2001). The NRLEUV model has been parameterized to use the F10.7 and Mg II core-to-wing index as solar proxy inputs.

The HFG (SERF1) model was based on rocket measurements for the detailed spectrum calibration and the Atmosphere Explorer measurements from solar minimum in mid 1977 until solar maximum in 1980 for scaling with solar activity (Hinteregger et al., 1981). The HFG model adopts a solar minimum spectrum (SC#21REF) and uses proxy indices to extrapolate to higher levels of solar activity. Each line in the spectrum is scaled individually as a linear function of the daily F10.7 index and the 81-day average F10.7 index with its own set of coefficients. Irradiances originating from the solar corona have a different variation from irradiances originating from the chromosphere. One anomaly with the HFG model is that most of the solar activity scaling factors do not automatically go to unity at solar minimum. The chromospheric irradiances remain greater than one at solar minimum while the coronal irradiances would be less than unity, except that they are set to unity when this happens (Richards and Torr, 1984). Tobiska and coworkers have developed a series of empirical EUV irradiance models related to the SERF1 model. These models include SERF2 by Tobiska and Barth (1990) EUV91 by Tobiska (1991), EUV97 by Tobiska and Eparvier (1998), and SOLAR2000 by Tobiska et al. (2000). These models evolved with the inclusion of additional data sets and more sophisticated fitting methods.

The solar EUV irradiance model for aeronomic calculations (EUVAC) was developed in response to a perceived need for a simple EUV irradiance model for calculating upper atmosphere densities and temperatures and also to correct an apparent problem with the solar reference irradiances below 25 nm that showed up as a discrepancy in the shape of theoretical and measured photoelectron flux spectra (Richards and Torr, 1984). The EUVAC model combined the F74113 standard EUV irradiance spectrum with the solar cycle relative variation observed by the AE-E satellite from day 183 of 1977 until day 365 of 1980. The F74113 solar EUV irradiances short ward of 25 nm (soft X-rays) were increased by a factor of 2–3 in order to produce good agreement between the shapes of the observed and modeled ionospheric photoelectron flux spectrum. The HFG irradiances also need to be scaled by a similar amount to bring modeled and measured photoelectron fluxes into agreement. The solar maximum results in this paper support the need to increase the model irradiances below 25 nm that was initially found at solar minimum. Recent satellite measurements of solar EUV irradiances also appear to support the larger soft X-ray irradiance in the EUVAC model. The adjustment below 25 nm produces the measured shape of the photoelectron spectrum while having little effect on the overall photoionization rate (Richards et al., 1994). Thus, the EUVAC solar irradiances are compatible with the basic chemical scheme that was developed from the Atmosphere Explorer-C satellite data. The EUVAC model also overcame the problem of the solar activity factors at solar minimum by forcing them to go to one for the solar activity corresponding to mid 1977 when the activity level was similar to 23 April 1974.

The increase in the irradiance below 25 nm in the EUVAC model was based on the need to reproduce the shape of the photoelectron flux that was measured on the Atmosphere Explorer-E satellite (Lee et al., 1980). The photons below 25 nm produce photoelectrons with energies above 35 eV. Without doubling the solar irradiance below 25 nm there is discontinuity near 35 eV in the theoretical photoelectron spectrum. While there still may be concern over the overall magnitude of the measured photoelectron flux, the shape of the spectrum is well established by several different instruments. Detailed Atmosphere Explorer photoelectron fluxes were only for solar minimum and there has been a lack of comparisons between measured photoelectron fluxes and photoelectron fluxes calculated using the EUVAC model solar irradiance at solar maximum.

Fortunately, good quality photoelectron spectra were measured on the FAST satellite on 21 April 2002 when SEE also measured the solar irradiance. As described in Woods et al. (2003), the FAST photoelectron data interval were selected to be well equatorward of precipitating auroral electrons, and away from the peak of the outer radiation belt region and its associated penetrating radiation environment. Spacecraft generated photoelectrons that are observed near 90° pitch angle are not included in the spectra. In addition, a small background signal has been subtracted from the data. Improved instrumental signal to noise characteristics extend the energy range for the FAST photoelectron measurements to about 1000 eV. This high sensitivity was obtained by careful design, multiple sensors, avoidance of the known sources of noise from spacecraft, and averaging over long 2-min intervals.

The photoelectron flux model used in this paper is imbedded in the field line interhemispheric plasma (FLIP) model (Richards, 2004). The FLIP model provides the background ionosphere and plasmasphere. The photoelectron flux model is based on the two-stream formulation of Nagy and Banks (1970) in which the photoelectron flux is divided into upward and downward components. The numerical procedure is similar to the procedure for auroral electron precipitation in the paper by Richards and Torr (1990). That paper also gives the electron impact cross-sections that are employed in the model. The model uses the photoionization cross-sections of Fennelly and Torr (1992) to calculate photoelectron production rates.

This paper examines the similarities and differences between the SEE measured and the modeled EUV irradiances for 21 April 2002. It also compares measured photoelectron fluxes with model photoelectron fluxes calculated with different solar EUV irradiances to show that the solar irradiance is consistent with the shape of the measured photoelectron flux spectrum.

2. HEUVAC: high resolution solar EUV irradiance model

The EUVAC model is still adequate for calculating aeronomic photoionization rates but its resolution is too coarse for photoelectron flux models. Also, the EUVAC model cannot produce photoelectrons with energies above 250 eV because there is no solar irradiance below 5 nm. These high energy photoelectrons are important for the photochemistry near 100 km in the E-region of the ionosphere.

The new high-resolution model (HEUVAC) has flexible wavelength binning to allow a better comparison of the irradiances with the measurements and other models that are of higher resolution than the EUVAC irradiances. The HEUVAC bins can range from 0.1 to 100 nm. The NRLEUV and SEE irradiances are typically plotted at 1 or 5 nm resolution. The EUVAC model has twenty 5 nm bins together with 17 individual lines for the strongest irradiances. HEUVAC does not separate the strong solar lines because this is not necessary for high resolution spectra. Solomon and Qian (2005) have produced a low resolution model that still provides accurate photoionization rates. With regard to solar activity scaling, it would be possible to provide new individual scaling factors for each HEUVAC bin but the EUVAC solar activity scaling factors were retained so that EUVAC based irradiances can be compared with measurements and other models.

The HEUVAC model takes the F74113 solar spectrum as the solar minimum reference spectrum with the 15–25 nm irradiances doubled and the 2.5–15 nm irradiances tripled. Below 2.5 nm the F74113 solar irradiances were increased by a factor of 9 based on the comparison of the measured and modeled photoelectron fluxes in this paper. When constructing the HEUVAC model it was found that the irradiances of the discrete lines were identical to the values of Torr et al. (1979) but discrepancies were noticed between some of the 5 nm bin values in Torr et al. (1979) values and the earlier values of Heroux and Hinteregger (1978). Our summing of the F74113 spectra into Torr et al. (1979) 37 eV bins also found discrepancies between 50 and 80 nm. For consistency between EUVAC and HEUVAC, the F74113 irradiances were scaled to agree with the EUVAC irradiances using the following factors: 50–55 nm (1.18), 55–60 nm (1.9), 60–65 nm (1.65), 65–70 nm (1.7), 70–75 nm (1.1), 75–80 nm (1.12).

The EUVAC and HEUVAC irradiances are effectively normalized to 1 AU because the F74113 spectrum is based on a rocket measurement on 23 April 1974 when the Sun–Earth distance was close to 1 AU. The variation in solar radiation because of the eccentricity of the Earth's orbit results in a ~3.5% greater solar irradiance on January 3 (perihelion) and ~3.5% lesser irradiance on July 4 (aphelion). The EUVAC and HEUVAC models should be corrected for Sun–Earth distance. However, in modeling the ionosphere and thermosphere, this variation is small compared to natural fluctuations in the solar irradiances and uncertainties in thermospheric densities and temperatures.

The F74113 spectrum lists the important solar lines and continuum irradiances. The spectrum resolution is basically 0.1 nm above 40 nm but less than 0.1 nm below 40 nm, which is much higher than is needed for most aeronomic calculations. The uncertainties in the EUVAC and HEUVAC models depend on the uncertainties in the F74113 irradiances and also on the way the irradiances are fitted as a linear function of the proxy $P = (F10.7A + F10.7)/2$ where $F10.7$ is the daily value of the 10.7 cm solar radio flux and $F10.7A$ is the 81-day average of daily $F10.7$ centered on the current day. An estimate of the latter error can be obtained from plots in the EUVAC paper that show the scatter in the data about the least squares fits (Richards et al., 1994). These plots show that on any particular day, the error in the EUVAC model, due to scatter in the data, can be as large as 30% but is generally less than 15%. Numerous studies of the ionosphere have shown that the EUVAC model irradiances produce satisfactory agreement with measured ionospheric quantities. In particular, Richards (2002) showed that the EUVAC model irradiances reproduced the observed altitude profiles of the electron and ion temperatures as well as the O_2^+, NO^+, O^+ densities on September 12, 1974. The EUVAC solar irradiances are also able to reproduce the basic solar cycle variation of the ionospheric peak density very well (Richards, 2001).

The HEUVAC model uses the HFG model for solar activity scaling by calculating average irradiances over the 0–5 nm bin for solar minimum and solar maximum. The calculated HFG solar cycle variation is consistent with the SEE 0–7 nm variation given by Woods et al. (2005). The HFG 0–5 nm solar irradiance varies by a factor of ~6 when the proxy P goes from 80 to 200. The SEE 0–7 nm irradiance varies by a factor of ~4 when P goes from ~95 to ~180.

A FORTRAN code of HEUVAC is available from the author. The model also provides irradiance weighted values of Fennelly and Torr (1992) photoionization cross-sections in the same wavelength bins for use in calculating ionospheric photoionization rates.

3. Results

3.1. Solar EUV irradiance comparisons

Fig. 1 shows a comparison of the HEUVAC, HFG, and SEE irradiances at 2 nm resolution for 21 April 2002. The 2 nm resolution was chosen here because it is fine enough to show the salient features of the EUV irradiance spectrum and coarse enough to reveal the key similarities and differences between the different irradiances.

For discussion purposes, it is convenient to divide the spectrum into three regions: (1) 2–35 nm that is the most important for photoelectron production; (2) 36–75 nm where the discrepancies between SEE and HEUVAC are largest; (3) 75–105 nm where the H Lyman continuum emissions are important.

In the region below 35 nm there are some bins where the HEUVAC irradiances are higher and some bins where the SEE irradiances are higher. This leads to generally good overall agreement in the total energy and number of photons below 35 nm. Because the SEE results shortward of 27 nm are based on scaling a reference spectrum (Woods et al., 2005) to match the broadband measurements, the agreement with the overall SEE irradiance magnitude is more important than individual bins.

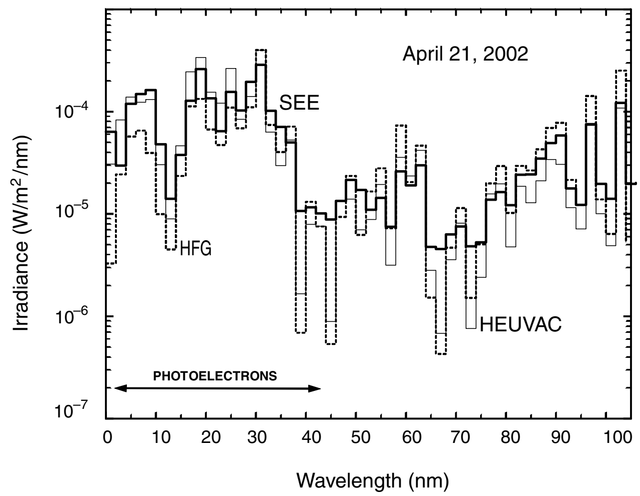

Between 35 and 75 nm there is reasonable agreement in the bins that feature strong spectral lines but large differences in the bins where there are no strong features in the F74113 reference spectrum, which is the basis of HEUVAC. This difference is most likely related to how the grating scattered light is corrected in the AE-E based reference spectrum and/or the SEE spectrum (Woods et al., 2005). In the 75–105 nm region there is also good agreement between HEUVAC and SEE irradiances in bins containing strong solar features but, in H Lyman continuum region between 80 and 90 nm, the SEE irradiances are a factor of 1.5 higher than the HEUVAC irradiances. Lean et al. (2003) noted similar discrepancies between the SC#21REFW spectrum and the NRLEUV reference spectrum.

There is generally good agreement between the HEUVAC and the HFG irradiances above 30 nm but the HEUVAC irradiances are a factor of 2–3 larger below 30 nm primarily because of the adjustment that was made to reproduce the shape of the measured photoelectron spectrum. In the H continuum region between 80 and 90 nm, the HFG irradiances are a factor of 1.5 higher than the HEUVAC irradiances and in good agreement with the SEE irradiances.

Fig. 2 shows the SEE spectrum at 1 nm resolution in the wavelength range 0–40 nm that is most important for photoelectron flux production. The HEUVAC spectrum is shown at 0.5 nm because this is the resolution that is used in calculating the Auger electron production between 20 and 35 eV. Breaks in the step function indicate bins with very low irradiances. At this higher resolution there is still generally good overall agreement

The photoelectron fluxes from the SEE and HEUVAC models generally agree to within 30% with each other and also with the FAST measurements up to 250 eV. More importantly, the shapes of the photoelectron model spectra when using the SEE and HEUVAC irradiances agree well with the measured spectral shape. Above 250 eV, the HFG and SEE based model photoelectron fluxes fall below the FAST measurements. There is little significance in the fact that the HEUVAC model gives better agreement with the photoelectron fluxes than the SEE measurements above 250 eV because the scaling is arbitrary. The original factor of 3 scaling between 5 and 15 nm was based on comparisons with the AE-E photoelectron spectrum below 100 eV only. The photoelectron fluxes obtained using the HFG irradiances demonstrate the magnitude of the problem with the unadjusted SC#21REFW reference irradiances below 25 nm. The HFG derived photoelectron fluxes agree well with the FAST data below 25 eV, but there are factor of 2 differences near 40 eV and factors of 3 differences above 60 eV. This result is consistent with the previous findings from comparisons between modeled and measured photoelectron fluxes for solar minimum conditions by Richards and Torr (1984). It is worth noting that, if the SC#21REFW irradiances are scaled below 25 nm using the EUVAC factors of 2–3, the HFG derived photoelectron fluxes are brought into good agreement with the HEUVAC derived photoelectron fluxes. It is also important to realize that photons with wavelengths above about 31 nm (~40 eV) have a relatively small effect on the photoelectron flux (Richards and Torr, 1984). This is because this solar irradiance is relatively small compared to the strong 30.4 nm irradiance and also because the photoelectrons that are produced by longer wavelength photons have energies less than ~20 eV where they are swamped by electrons cascading from higher energies.

Photoelectrons with energies above 250 eV are generated by photons with wavelengths below 5 nm. The HEUVAC and HFG irradiances are very uncertain below 5 nm for several reasons: (1) there is a lack of measured irradiances that contribute to the F74113 and SC#21REFW reference spectra; (2) there are no measurements of the solar cycle variation from AE-E; (3) the photoionization cross-sections are highly structured. Winningham et al. (1989) and FAST photoelectron measurements show that the Auger process is very important and that the 2–3.5 nm irradiance is large. Thus, the F74113 irradiances below 2.5 nm were adjusted to bring the HEUVAC modeled photoelectron fluxes into better agreement with the FAST measured photoelectron fluxes. The calculated Auger electron flux near 500 eV is very sensitive to the irradiance in a narrow region near 2.3 nm where the O photoionization cross-section peaks. On the other hand, the photoelectron flux near 360 eV is more sensitive to the irradiance between 2.5 and 3 nm where the N_2 photoionization cross-section peaks.

There are two factors that may contribute to the discrepancy in this energy region when using the SEE EUV irradiances. First, it is the most dynamic region of the solar spectrum and 21 April 2002 was an active day with solar flare activity. The FAST fluxes were not taken at the exact time of the SEE irradiances and there may have been some enhanced EUV irradiance at this time. Second, there is uncertainty in the assumed spectral shape that is used to interpret the SEE broadband measurements in this region of the solar spectrum. There would be much better agreement if the assumed spectrum distributed more of the SEE irradiance between 2 and 3.5 nm. This uncertainty in the spectral shape is expected to be largest during solar flare activity.

Woods et al. (2003) also compared model photoelectron fluxes with fluxes measured by the FAST satellite for 21 April 2002. The present comparison differs from the earlier calculation in that the model photoelectron fluxes are calculated at the satellite altitude, the fluxes are shown below 20 eV, and this paper uses the latest version of the SEE solar EUV irradiances. In Woods et al. (2003) paper, the model photoelectron fluxes were in close agreement above 100 eV and below 30 eV, but between 30 and 100 eV the model photoelectron fluxes were much lower than the current model fluxes.

Because the satellite photoelectron fluxes are measured well above the region where the photoelectrons are created, it is important to examine the altitude variation of the flux as it travels from the ionosphere to the plasmasphere. Fig. 4 shows how the model upward field aligned photoelectron flux spectrum changes with altitude. At solar maximum, transport effects are still small up to 400 km but become more important with increasing altitude. The

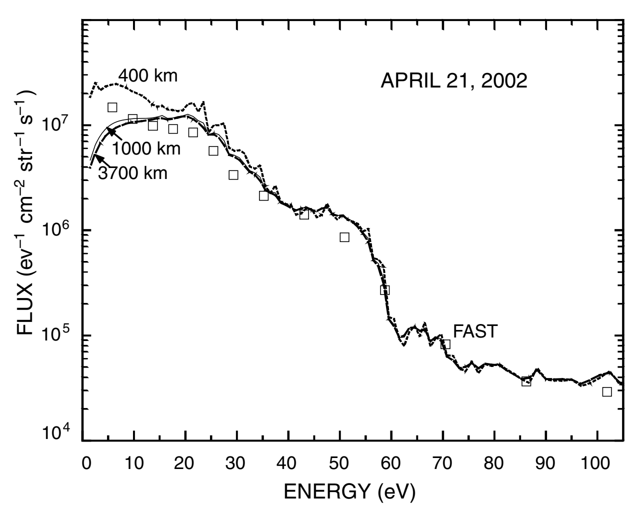

Fig. 4. Comparison of modeled photoelectron fluxes at 400 km (short dashed line), 1000 km (solid line), and 3700 km (long dashed line). The FAST measurements (squares) are at 3700 km. All three model calculations use the HEUVAC model solar irradiances.

400 km spectrum that is shown in Fig. 4 reveals the characteristic 20–30 eV peaks in the spectrum caused by the relatively intense 30.4 nm solar EUV flux. The ionospheric photoelectrons are degraded by Coulomb collisions with thermal electrons as they travel along magnetic field lines from the ionosphere to the FAST satellite at 3700 km. The degradation is small above 30 eV but the lower the energy, the greater the degradation, and it is particularly severe below 20 eV. The Coulomb collisions also cause the peaks to be washed out.

Fig. 4 shows that most of the degradation takes place in the topside ionosphere below 1000 km for the solar maximum conditions on 21 April 2002. There is some uncertainty over the topside electron densities, which are calculated using the FLIP model. Comparisons at Hobart (43S, 147E) indicate that the model electron density is about 30% higher than was measured by the ionosonde for the same local time on 21 April 2002. Since this is a period of intense magnetic activity, the model may overestimate the peak electron density near 400 km. However, parameter studies with modified inputs to change the electron density did not significantly change the results because the photoelectron flux is sensitive to the integrated electron density, which also depends on plasma temperature. Electron density and temperature are anticorrelated in the topside ionosphere so that smaller electron densities are counterbalanced to a certain extent by higher temperatures with regard to the integrated density.

3.3. Airglow production rate comparison

It is very important to establish accurate emission rates as these emissions are commonly used to deduce key characteristics of the thermosphere (Strickland et al., 2004). Fig. 5 shows how the different solar irradiance models affect the calculated OI 135.6 nm and the N_2 Lyman–Birge–Hopfield (LBH) airglow emission rates that are obtained by folding the photoelectron flux with the partial cross-section and neutral density. The calculated emission rates from the SEE and HEUVAC models are similar but the HFG production rates are ~50% lower. The EUV irradiances can also have an effect on the ratios of the OI 135.6 and LBH emissions that are commonly used for determining the O to N_2 density ratio in the thermosphere. The ratios of the LBH peak production to 135.6 peak production are 6.4 for the HFG irradiances, 6.8 for the SEE irradiances, and 7.4 for HEUVAC irradiances. Thus, an inaccurate solar EUV irradiance spectrum can lead to inaccuracies in calculated neutral density ratios.

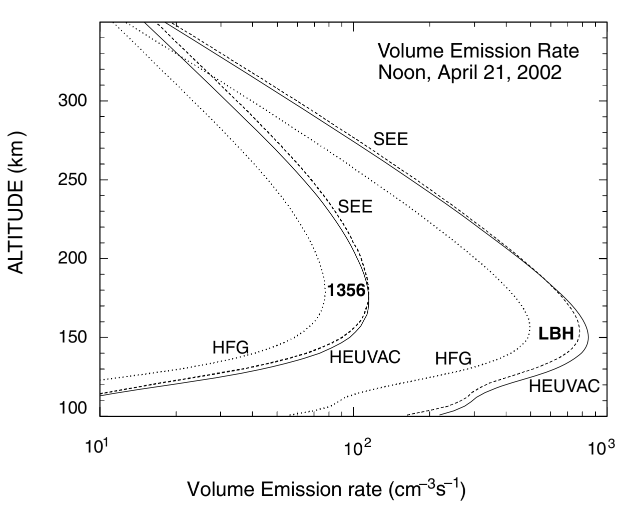

Fig. 5. Comparison of modeled OI 1356, and total N_2 LBH airglow production rates using HEUVAC (solid line), HFG (dotted lines), SEE (dashed line) solar EUV irradiances.

4. Conclusion

This paper presents a new high-resolution version of the EUVAC model (HEUVAC) to improve accuracy and facilitate comparisons with recent solar EUV irradiance measurements. The solar EUV irradiance comparisons in this paper show good overall agreement between the HEUVAC model and the SEE version 8 measurements. However, there are differences in the details. The shapes of the measured and modeled photoelectron fluxes are compared as a cross-check on the solar EUV irradiances below ~40 nm. The photoelectron flux comparisons that are shown in this paper support earlier studies that indicated the need to increase the solar EUV irradiances below 25 nm in the F74113 and SC21REFW solar EUV reference spectra. The photoelectron fluxes produced from the HEUVAC solar EUV irradiances are in good agreement below 200 eV and therefore result in excellent agreement in ion production, electron heating, and airglow emission rates. Above 200 eV where the Auger process is dominant, there is much more uncertainty in the solar irradiance and therefore in the calculated photoelectron fluxes. The 300–500 eV photoelectron flux suggests that the 2–3.5 nm irradiance needs to be around $10^{-4}\,W\,m^{-2}s^{-1}nm^{-1}$ on 21 April 2002, which corresponds to an order of magnitude increase in the F74113 and SC#21REFW reference irradiances in this region. The photoelectron flux from the SEE measurements could be brought into agreement with the FAST measurements either by a factor of 3–4 increase in the 2–3.5 nm irradiance, or by redistributing the large 1–2 nm irradiance to the 2–3.5 nm wavelength region. The difference in the various irradiances are important because airglow emission rates from the HFG solar irradiance model are about 50% lower than those calculated with the HEUVAC and SEE irradiances.

Acknowledgments

This work was carried out under NASA Grant IPA022 to the University of Alabama in Huntsville and under NASA Grant NAG5-11408 to the University of Colorado.

References

Avakyan, S.V., Vlasov, M.N., Krinberg, I.A. Comparisons of the fluxes and spectra of auger electrons and photoelectrons in the Earth's ionosphere and plasmasphere. Geomagn. Aeron. 17, 54, 1977.

Bailey, S.M., Barth, C.A., Solomon, S.C. A model of nitric oxide in the lower thermosphere. J. Geophys. Res. 107 (A8), 1205, doi:10.1029/2001JA000258, 2002.

Berkowitz, J. Photoabsorption, Photoionization, and Photoelectron Spectroscopy. Academic Press, San Diego, CA, 1979.

Fennelly, J.A., Torr, D.G. Photoionization and photoabsorption cross-sections of O, N_2, O_2 and N for aeronomic calculations. Atom. Data Nucl. Data Tables 51, 321–363, 1992.

Fontenla, J.M., White, O.R., Fox, P.A., Avrett, E.H., Kurucz, R.L. Calculation of solar irradiances. I. Synthesis of the solar spectrum. Astrophys. J. 518, 480, 1999.

Gorczyca, T.W., McLaughlin, B.M. J. Phys. B 33, L859–L863, 2000, S0953-4075(00)50571-9.

Heroux, L., Hinteregger, H.E. Aeronomical reference spectrum for solar UV below 2000 Å. J. Geophys. Res. 83, 5305, 1978.

Hinteregger, H.E., Fukui, K., Gilson, B.R. Observational, reference and model data on solar EUV, from measurements on AE-E. Geophys. Res. Lett. 8, 1147, 1981.

Lean, J.L., Livingston, W.C., Heath, D.F., Donnelly, R.F., Skumanich, A., White, O.R. A three-component model of the variability of the solar ultraviolet flux 145–200 nm. J. Geophys. Res. 87, 10307, 1982.

Lean, J.L., Warren, H.P., Mariska, J.T., Bishop, J. A new model of solar EUV irradiance variability: 2. Comparisons with empirical models and observations and implications for space weather. J. Geophys. Res. 108 (A2), 1059, doi:10.1029/2001JA009238, 2003.

Lee, J.S., Doering, J.P., Potemra, T.A., Brace, L.H. Measurements of the ambient photoelectron spectrum from Atmosphere Explorer, I, AE-E measurements below 300 km during solar minimum conditions. Planet. Space Sci. 28, 947, 1980.

Nagy, A.F., Banks, P.M. Photoelectron fluxes in the ionosphere. J. Geophys. Res. 75, 6260, 1970.

Richards, P.G. Seasonal and solar cycle variations of the ionospheric peak electron density: comparison of measurement and models. J. Geophys. Res. 106, 12803, 2001.

Richards, P.G. Ion and neutral density variations during ionospheric storms in September1974: comparison of measurement and models. J. Geophys. Res. 107 (A11), 1361, doi:10.1029/2002JA009278, 2002.

Richards, P.G. On the increases in nitric oxide density at mid latitudes during ionospheric storms. J. Geophys. Res. 109, A06304, doi:10.1029/2003JA010110, 2004.

Richards, P.G., Torr, D.G. A simple theoretical model for calculating and parameterizing the ionospheric photoelectron flux. J. Geophys. Res. 88, 2155, 1983.

Richards, P.G., Torr, D.G. An investigation of the consistency of the ionospheric measurements of the photoelectron flux and solar EUV flux. J. Geophys. Res. 89, 5625, 1984.

Richards, P.G., Torr, D.G. Theoretical modeling of the dependence of the N_2 second positive 3371 Å auroral emission on characteristic energy. J. Geophys. Res. 95, 10337–10344, 1990.

Richards, P.G., Fennelly, J.A., Torr, D.G. EUVAC: a solar EUV flux model for aeronomic calculations. J. Geophys. Res. 99, 8981, 1994.

Solomon, S.C., Qian, L. Solar extreme-ultraviolet irradiance for general circulation models. J. Geophys. Res. (in press).

Stolte, W.C., Lu, Y., Samson, J.A.R., Hemmers, O., Hansen, D.L., Whitfield, S.B., Wang, H., Glans, P., Lindle, D.W. The K-shell Auger decay of atomic oxygen. J. Phys. B 30, 4489–4497, 1997.

Strickland, D.J., Meier, R.R., Walterscheid, R.L., Craven, J.D., Christensen, A.B., Paxton, L.J., Morrison, D., Crowley, G. Quiet-time seasonal behavior of the thermosphere seen in the far ultraviolet dayglow. J. Geophys. Res. 109, A01302, doi:10.1029/2003JA010220, 2004.

Tobiska, W.K., Eparvier, F.G. EUV97: improvements to EUV irradiance modeling in the soft X-rays and FUV. Solar Phys. 177, 147, 1998.

Tobiska, W.K., Barth, C.A. A solar EUV flux model. J. Geophys. Res. 95, 8243–8251, 1990.

Tobiska, W.K., Woods, T.N., Eparvier, F.G., Viereck, R., Floyd, L., Bouwer, D., Rottman, G.J., White, O.R. The SOLAR2000 empirical solar irradiance model and forecast tool. J. Atmos. Sol.-Terr. Phys. 62, 1233, 2000.

Tobiska, W.K. Revised solar extreme ultraviolet flux model. J. Atmos. Terr. Phys. 53, 1005, 1991.

Torr, M.R., Torr, D.G., Ong, R.A., Hinteregger, H.E. Ionization frequencies for major thermospheric constituents as a function of solar cycle 21. Geophys. Res. Lett. 6, 771, 1979.

Warren, H.P., Mariska, J.T., Lean, J. A new reference spectrum for the EUV irradiance of the quiet Sun: 1. Emission measure formulation. J. Geophys. Res. 103, 12077, 1998a.

Warren, H.P., Mariska, J.T., Lean, J. A new reference spectrum for the EUV irradiance of the quiet Sun: 2. Comparisons with observations and previous models. J. Geophys. Res. 103, 12091, 1998b.

Warren, H.P., Mariska, J.T., Lean, J. A new model of solar EUV irradiance variability: 1. Model formulation. J. Geophys. Res. 106, 15745, 2001.

Winningham, J.D., Decker, D.T., Kozyra, J.U., Jasperse, J.R., Nagy, A.F. Energetic (>60 eV) atmospheric photoelectrons. J. Geophys. Res. 94, 15335–15348, 1989.

Woods, T.N., Bailey, S.M., Peterson, W.K., Warren, H.P., Solomon, S.C., Eparvier, F.G., Garcia, H., Carlson, C.W., McFadden, J.P. Solar extreme ultraviolet variability of the X-class flare on 21 April 2002 and the terrestrial photoelectron response. Space Weather 1 (1), 1001, doi:10.1029/2003SW000010, 2003.

Woods, T.N., Eparvier, F.G., Fontenla, J., Harder, J., McClintock, G.W.E., Rottman, G., Smiley, B., Snow, M. Solar irradiance variability during the October 2003 solar storm period. Geophys. Res. Lett. 31, L10802, doi:10.1029/2004GL019571, 2004.

Woods, T.N., Eparvier, F.G., Bailey, S.M., Chamberlin, P.C., Lean, J., Rottman, G.J., Solomon, S.C., Tobiska, W.K., Woodraska, D.L. Solar EUV experiment (SEE): mission overview and first results. J. Geophys. Res. 110, A01312, doi:10.1029/2004JA010765, 2005.